INTERNATIONAL JOURNAL OF TECHNOLOGY AND ACADEMIC RESEARCH

ISSN: 2224-6878 | Pakistan Volume 6, No. 10.

IF: 14.91 | 2026 http://waerasia.org/index.php/ijtar

FREE-ION GROUND STATE, EFFECTIVE AXIAL CRYSTAL FIELD AND SINGLE-ION MAGNETOTHERMAL PROPERTIES OF THE Dy^{3+} ION IN ORTHOALUMINATE $DyAlO_3$

Saidov Kurbon Sayfulloevich
Candidate of Physical and Mathematical Sciences, Associate Professor,
Bukhara State University, Bukhara, Uzbekistan
qurbonsaid@mail.ru

Usmonova Bakhtiniso Sharif qizi
Lecturer, Department of Exact Sciences,
Bukhara State Technical University, Bukhara, Uzbekistan
usmonova.baxtinis93@gmail.com
https://doi.org/10.5281/zenodo.23243713

Abstract. The Dy^{3+} ion in dysprosium orthoaluminate $DyAlO_3$ is a Kramers ion with one of the largest magnetic moments in the lanthanide series, but its single-ion properties have mostly been described qualitatively. This work builds a quantitative chain from free-ion theory to measurable thermodynamic quantities. Hund's rules and LS coupling give the ground term $^6H_{15/2}$, the Landé factor $g_J = 4/3$ and the effective moment $\mu_{eff} = 10.65\ \mu_B$, the highest among the trivalent lanthanides. The energies of the four lowest Kramers doublets of $^6H_{15/2}$ (0, 53.7, 125.7 and 205.5 cm^{-1}), obtained from the Stark structure of the $^6H_{15/2} \rightarrow {}^6F_{3/2}$ absorption band, were fitted with an effective axial crystal-field Hamiltonian in Stevens operators. A second-order term alone ($B_2^0 = -1.75$ cm^{-1}) leaves an rms deviation of 16.1 cm^{-1}. Adding the fourth-order term ($B_2^0 = -2.55$ cm^{-1}, $B_4^0 = 2.45\times10^{-3}$ cm^{-1}) reduces it to 0.24 cm^{-1}, confirms the $|\pm15/2\rangle$ ground doublet and places the four unresolved doublets at 281–416 cm^{-1}. From this level scheme, the Schottky heat capacity, the magnetic entropy and the magnetization were calculated. The heat-capacity maximum shifts from 57 K (four resolved doublets) to 118 K (complete scheme), which offers a direct calorimetric test of the predicted upper levels. At 10 K and 1 T the Ising doublet gives 5.87 μ_B along its axis, compared with 2.46 μ_B for a free ion and 2.06 μ_B for a powder average. The results provide a consistent single-ion basis for interpreting the magnetic anisotropy and the magnetocaloric potential of $DyAlO_3$.

Keywords: dysprosium orthoaluminate, Dy^{3+}, Hund's rules, Landé factor, crystal field, Stevens operators, Kramers doublets, Ising anisotropy, Schottky anomaly, magnetic entropy, magnetization.

Introduction. Rare-earth (RE) orthoaluminates $RAlO_3$ are convenient model systems for single-ion magnetism: the RE ion occupies a low-symmetry site (point group C_s), the 4f shell is well shielded by the filled $5s^25p^6$ shells, and the crystal field (CF) is weak compared with the spin–orbit interaction [1, 2]. Under these conditions each free-ion multiplet J splits into a small number of Stark sublevels whose wave functions control the magnetic and optical response of the crystal [3, 4].

Among these compounds, $DyAlO_3$ stands out. Dy^{3+} ($4f^9$) has an odd number of electrons, so by Kramers' theorem every Stark level remains a doublet in the absence of a magnetic field [5]. The large uniaxial component of the CF makes the ground doublet close to the state $|\pm15/2\rangle$, which gives it an extremely anisotropic, Ising-type g-tensor [1, 6, 7]. The magnetic susceptibility

ISSN: 2224-6878 | Pakistan Volume 6, No. 10.

IF: 14.91 | 2026 http://waerasia.org/index.php/ijtar

of $DyAlO_3$ remains anisotropic up to T > 100 K, which suggests that the Ising character extends to the excited doublets of the ground multiplet [1].

Previous studies of $DyAlO_3$ established the main qualitative features of its energy spectrum but did not connect the measured Stark energies to a CF model or to thermodynamic quantities that can be checked independently [1, 8]. Polarization effects and magneto-optical applications are treated separately in [8]. The present work addresses a different question: how far a minimal, physically transparent model can reproduce the measured level scheme, and what this model predicts for heat capacity, entropy and magnetization.

The aim of the work is to build a quantitative single-ion description of Dy^{3+} in $DyAlO_3$, from the free-ion ground state through the CF level scheme to measurable magnetothermal properties. The objectives are:

– to derive the ground term, Landé factor and magnetic moments of Dy^{3+} from Hund's rules and to place them within the heavy-lanthanide series;

– to fit the measured energies of the lowest Kramers doublets with an effective axial CF Hamiltonian and to test the $|\pm 15/2\rangle$ ground state;

– to predict the energies of the unresolved doublets of $^6H_{15/2}$;

– to calculate the Schottky heat capacity, magnetic entropy and field dependence of the magnetization;

– to formulate experimental tests of the model.

Materials and methods. Experimental data. The object of study is single-crystal dysprosium orthoaluminate $DyAlO_3$, in which Dy^{3+} occupies a C_s site of the orthorhombic structure [1]. The input data are the energies of the eight Stark components of the $^6H_{15/2} \rightarrow {}^6F_{3/2}$ absorption band, recorded in two orthogonal polarizations at low temperature, and their assignment to transitions from the four lowest Kramers doublets (I–IV) of $^6H_{15/2}$ to the two doublets (a, b) of $^6F_{3/2}$ [8]. Earlier unpolarized measurements at 4.2 and 77 K were used for comparison [1]. The energy of each ground doublet relative to doublet I was taken as the mean of the values obtained from the a and b transition series.

Free-ion ground state. The ground term of the $4f^9$ configuration was determined in the LS-coupling scheme with Hund's rules [2, 9]: maximum total spin S; maximum total orbital momentum L compatible with S; and, for a shell more than half filled, J = L + S:

$$S=\sum m_s, \quad L=\left|\sum m_l\right|, \quad J=L+S \quad (n>7). \tag{1}$$

The Landé factor and the effective and saturation moments were calculated as

$$g_J=1+\frac{J(J+1)+S(S+1)-L(L+1)}{2J(J+1)}, \quad \mu_{eff}=g_J\sqrt{J(J+1)}\,\mu_B, \quad \mu_{sat}=g_J J\,\mu_B. \tag{2}$$

The fine-structure intervals within the ^6H term follow the Landé interval rule [2]:

$$E(J)-E(J-1)=\lambda J, \quad \lambda=-\frac{\zeta_{4f}}{2S}, \tag{3}$$

where ζ_{4f} is the spin–orbit coupling constant; the negative sign of λ for n > 7 places J = 15/2 lowest.

Effective axial crystal-field model. Because the CF splitting (~10^2 cm^{-1}) is two orders of magnitude smaller than the spacing between the ^6H_J multiplets (~10^3–10^4 cm^{-1}) [10, 11], the $^6H_{15/2}$ multiplet was treated as isolated. Its CF splitting was described with an effective axial Hamiltonian written in Stevens operator equivalents [4, 12], with the quantization axis along the local easy (Ising) axis:

$$H_{CF}=B_2^0O_2^0+B_4^0O_4^0, \tag{4}$$

$$O_2^0=3J_z^2-J(J+1), \quad O_4^0=35J_z^4-[30J(J+1)-25]J_z^2-6J(J+1)+3J^2(J+1)^2. \tag{5}$$

ISSN: 2224-6878 | Pakistan Volume 6, No. 10.

IF: 14.91 | 2026 http://waerasia.org/index.php/ijtar

The Hamiltonian (4) is diagonal in $|J, M\rangle$, so each doublet $|\pm M\rangle$ has energy $E(M) = B_2^0O_2^0(M) + B_4^0O_4^0(M)$. Assuming that the four lowest doublets are $|\pm 15/2\rangle$, $|\pm 13/2\rangle$, $|\pm 11/2\rangle$ and $|\pm 9/2\rangle$, the parameters were obtained by linear least squares from the three measured intervals $\Delta_K = E(M_K) - E(15/2)$. Two models were compared: model A with B_2^0 only (two degrees of freedom) and model B with B_2^0 and B_4^0 (one degree of freedom). The non-axial terms B_k^q ($q \neq 0$) allowed by C_s symmetry mix states with different M; they were neglected, so the fitted values are effective parameters.

Thermodynamic quantities. With the doublet energies E_i measured from the ground doublet, $\varepsilon_i = E_i/k_BT$ and $k_B = 0.6950$ cm^{-1}/K, the partition function, Schottky heat capacity and entropy per mole of Dy^{3+} are [13]

$$Z=\sum_i 2\exp(-\varepsilon_i), \quad C_{Sch}=R(\langle \varepsilon^2\rangle - \langle \varepsilon\rangle^2), \quad S=R(\ln Z+\langle \varepsilon\rangle). \tag{6}$$

The calculations were made for the four resolved doublets and for the complete eight-doublet scheme of model B. The magnetization at T = 10 K was calculated, neglecting exchange interactions, for the free ion (Brillouin function B_J), for an Ising $|\pm 15/2\rangle$ doublet with the field along its axis, and for an Ising doublet averaged over field directions (powder) [3, 14]:

$$M_{free}=g_J J\mu_B B_J(x), \quad M_{\parallel}=\mu_{\parallel}\tanh\frac{\mu_{\parallel}B}{k_BT}, \quad M_{pow}=\int_0^1 \mu_{\parallel} u \tanh\frac{\mu_{\parallel}Bu}{k_BT}du, \tag{7}$$

where $x = g_J J\mu_B B/k_BT$ and $\mu_{\parallel} = g_J M\mu_B = 10\ \mu_B$ for $M = 15/2$.

Results. Free-ion ground state. Removing the two 6s electrons and one 4f electron from the neutral atom ($[Xe]4f^{10}6s^2$) gives Dy^{3+} the configuration $[Xe]4f^9$, i.e. 63 electrons distributed over the shells as shown in Table 1. Only the partly filled 4f subshell carries a magnetic moment; the closed $5s^25p^6$ shells, which lie further out, screen it from the ligands [2].

Table 1. Electron configuration of the Dy^{3+} ion by shells

Shell	Subshells	Electrons
n = 1	$1s^2$	2
n = 2	$2s^22p^6$	8
n = 3	$3s^23p^63d^{10}$	18
n = 4	$4s^24p^64d^{10}4f^9$	27
n = 5	$5s^25p^6$	8
Total		**63**

Source: compiled by the authors.

Table 2 shows the application of Hund's rules (1). Seven electrons occupy the seven 4f orbitals ($m_l = -3\ldots+3$) with parallel spins; the remaining two have opposite spin and occupy $m_l = +3$ and +2. This gives S = 5/2, L = 5 (H) and, since the shell is more than half filled, J = 15/2. Equation (2) then gives $g_J = 4/3$, $\mu_{eff} = 10.65\ \mu_B$ and $\mu_{sat} = 10\ \mu_B$. By the interval rule (3), the ^6H_J levels lie above $^6H_{15/2}$ in the order J = 13/2, 11/2, 9/2, 7/2, 5/2, with successive intervals in the ratio 15 : 13 : 11 : 9 : 7.

Table 2. Determination of the ground term of Dy^{3+} ($4f^9$) by Hund's rules

Step	Rule	Result for $4f^9$
1	Maximize S: 7 electrons with spin up, 2 with spin down	S = 7/2 − 1 = 5/2; 2S + 1 = 6
2	Maximize L for this S: the 2 paired electrons in $m_l = +3, +2$	L = 3 + 2 = 5 (H)

ISSN: 2224-6878 | Pakistan Volume 6, No. 10.

IF: 14.91 | 2026 http://waerasia.org/index.php/ijtar

Step	Rule	Result for $4f^9$
3	Shell more than half filled: J = L + S	J = 15/2
4	Ground term	$^6H_{15/2}$
5	Landé factor, Eq. (2)	$g_J = 4/3$
6	Effective and saturation moments, Eq. (2)	$\mu_{eff} = 10.65\ \mu_B$; $\mu_{sat} = 10\ \mu_B$

Source: calculated by the authors.

Table 3 and Fig. 1 place Dy^{3+} among the heavy lanthanides. Its free-ion effective moment is the largest of the series (10.65 μ_B), marginally above that of Ho^{3+} (10.61 μ_B), and its saturation moment $g_JJ = 10\ \mu_B$ is shared only with Ho^{3+}. Unlike Ho^{3+} ($4f^{10}$, integer J), Dy^{3+} is a Kramers ion, so its doublet degeneracy cannot be lifted by the crystal field. The combination of a maximal moment with guaranteed doublet ground states is the physical basis for the strong Ising anisotropy of Dy compounds [6, 7].

Table 3. Ground terms and magnetic moments of the heavy trivalent lanthanide ions

Ion	Configuration	Ground term	g_J	μ_{eff}, μ_B	g_JJ, μ_B	Kramers ion
Gd^{3+}	$4f^7$	$^8S_{7/2}$	2	7.94	7	yes
Tb^{3+}	$4f^8$	$^7F_6$	3/2	9.72	9	no
Dy^{3+}	**$4f^9$**	**$^6H_{15/2}$**	**4/3**	**10.65**	**10**	**yes**
Ho^{3+}	$4f^{10}$	$^5I_8$	5/4	10.61	10	no
Er^{3+}	$4f^{11}$	$^4I_{15/2}$	6/5	9.58	9	yes
Tm^{3+}	$4f^{12}$	$^3H_6$	7/6	7.56	7	no
Yb^{3+}	$4f^{13}$	$^2F_{7/2}$	8/7	4.54	4	yes

Source: calculated by the authors with Eqs. (1) and (2).

ISSN: 2224-6878 | Pakistan Volume 6, No. 10.

IF: 14.91 | 2026 http://waerasia.org/index.php/ijtar

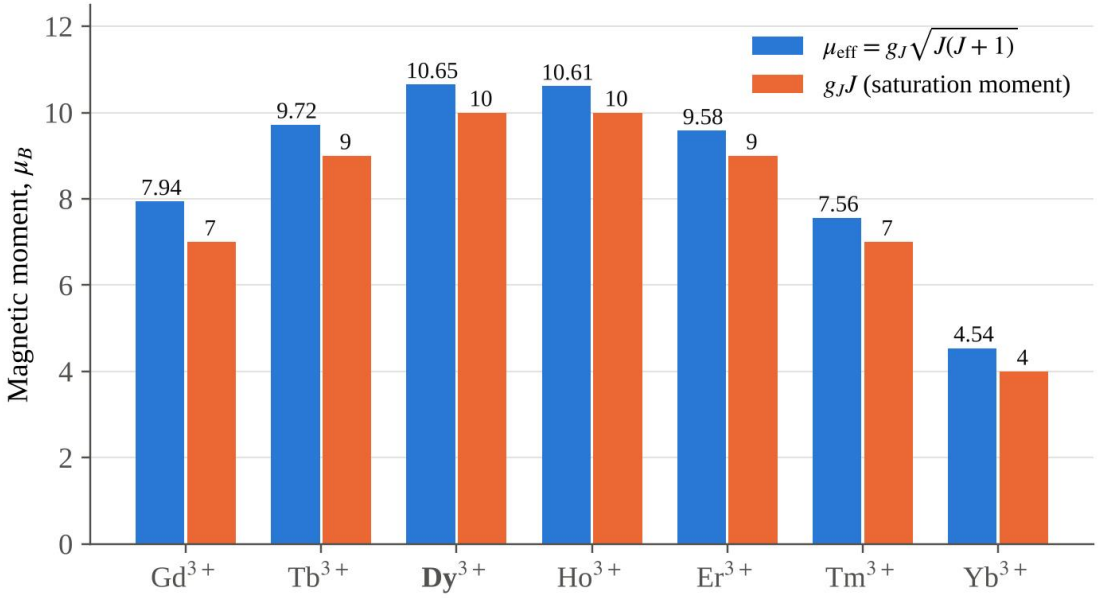


Figure 1. Free-ion effective moment μ_{eff} and saturation moment g_JJ of the heavy trivalent lanthanide ions. Calculated by the authors.

Stark structure and effective crystal field. Table 4 lists the Stark components of the $^6H_{15/2} \rightarrow {}^6F_{3/2}$ band and the resulting energies of doublets II–IV: 53.7, 125.7 and 205.5 cm^{-1}. The $^6F_{3/2}$ splitting averaged over the four ground doublets is 10.1 cm^{-1}. These values agree with the earlier estimates of 54 ± 2, 126 ± 2 and 208 ± 3 cm^{-1} obtained from unpolarized spectra [1].

Table 4. Stark components of the $^6H_{15/2} \rightarrow {}^6F_{3/2}$ band and energies of the ground-multiplet doublets

Ground doublet	Transition to a, cm^{-1}	Transition to b, cm^{-1}	Energy above doublet I, cm^{-1}
I	13 293.7	13 304.6	0
II	13 241.0	13 250.0	53.7
III	13 169.0	13 178.0	125.7
IV	13 088.0	13 099.4	205.5

Source: line positions from [8]; doublet energies are means of the a and b series.

The results of fitting the effective axial Hamiltonian (4)–(5) are given in Table 5 and Fig. 2. Model A (second-order term only) fails: with $B_2^0 = -1.75$ cm^{-1} it overestimates Δ_{II} by 20 cm^{-1} and underestimates Δ_{IV} by 16 cm^{-1} (rms deviation 16.1 cm^{-1}). A pure O_2^0 field produces intervals in the fixed ratio 42 : 78 : 108 (1 : 1.86 : 2.57), whereas the observed ratio is 1 : 2.34 : 3.83; the measured spacings grow with $|\Delta M|$ faster than a quadratic form in M allows. Model B, with the fourth-order term added, reproduces all three intervals to within 0.3 cm^{-1} (rms 0.24 cm^{-1}) with $B_2^0 = -2.55$ cm^{-1} and $B_4^0 = +2.45\times10^{-3}$ cm^{-1}. Both models give $B_2^0 < 0$, which makes $|\pm15/2\rangle$ the ground doublet and confirms its Ising character, with $g_{\parallel} = 2g_J \cdot 15/2 = 20$ and $g_{\perp} = 0$ [3].

Table 5. Observed and calculated energies (cm^{-1}) of the Kramers doublets of $^6H_{15/2}$ in the effective axial crystal-field model

Doublet	$\|\pm M\rangle$	Observed	Model A	Model B	Residual (B)
I	15/2	0	0	0	—

ISSN: 2224-6878 | Pakistan Volume 6, No. 10.

IF: 14.91 | 2026 http://waerasia.org/index.php/ijtar

Doublet	|±M⟩	Observed	Model A	Model B	Residual (B)
II	13/2	53.7	73.7	53.4	−0.3
III	11/2	125.7	136.9	126.0	+0.3
IV	9/2	205.5	189.5	205.3	−0.1
V	7/2	—	231.7	281.2	prediction
VI	5/2	—	263.2	345.3	prediction
VII	3/2	—	284.3	391.5	prediction
VIII	1/2	—	294.8	415.6	prediction
Parameters, cm^{-1}			**B_2^0 = −1.755**	**B_2^0 = −2.548; B_4^0 = 2.454×10^{-3}**	
rms, cm^{-1}			**16.1**	**0.24**	

Source: calculated by the authors with Eqs. (4) and (5); Stevens operator normalization [4, 12].

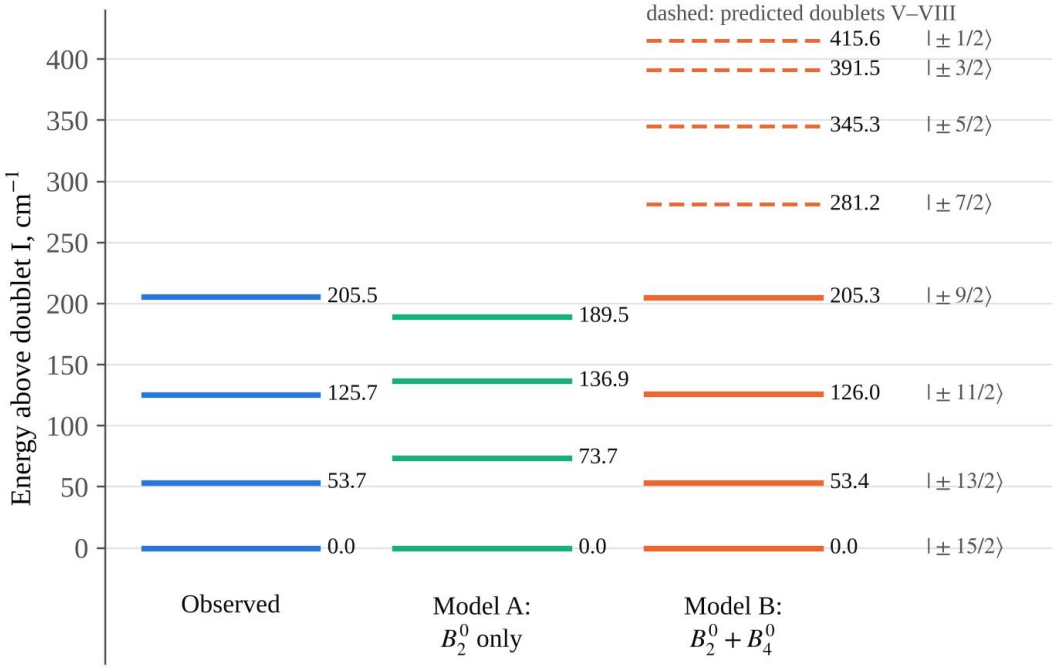


Figure 2. Energies of the Kramers doublets of $^6H_{15/2}$: observed (doublets I–IV) and calculated in the effective axial model with B_2^0 only (model A) and with B_2^0 + B_4^0 (model B). Calculated by the authors.

Model B predicts the four unresolved doublets V–VIII at 281, 345, 392 and 416 cm^{-1}, i.e. a total CF splitting of $^6H_{15/2}$ of about 416 cm^{-1}. The successive spacings in model B (53, 73, 79, 76, 64, 46 and 24 cm^{-1}) first grow and then shrink towards $|\pm1/2\rangle$. A pure second-order field would

ISSN: 2224-6878 | Pakistan Volume 6, No. 10.

IF: 14.91 | 2026 http://waerasia.org/index.php/ijtar

instead give spacings that decrease monotonically from the ground doublet upwards (in the ratio 7 : 6 : 5 : … : 1 for B_2^0 only, since E(M) ∝ M^2). The measured spacings of the lowest doublets (53.7, 72.0 and 79.8 cm^{-1}) increase, which is the direct reason for the failure of model A and the signature of the fourth-order term.

Heat capacity and entropy. The Schottky heat capacity and magnetic entropy calculated with Eq. (6) are shown in Fig. 3 and Table 6. Below 10 K only the ground doublet is populated, C_{Sch} vanishes and the entropy equals R ln 2 (5.76 J mol^{-1} K^{-1}), the value of an isolated Kramers doublet. Doublet II (53.7 cm^{-1} = 77 K) becomes populated above about 15 K, and the heat capacity rises steeply. With the four resolved doublets alone, C_{Sch} reaches a maximum of 5.38 J mol^{-1} K^{-1} at 57 K and the entropy tends to R ln 8. With the complete level scheme of model B, the maximum moves to 118 K and grows to 6.95 J mol^{-1} K^{-1}, and the entropy tends to R ln 16. The two curves coincide within 1% up to about 40 K and diverge strongly above 60 K (Table 6).

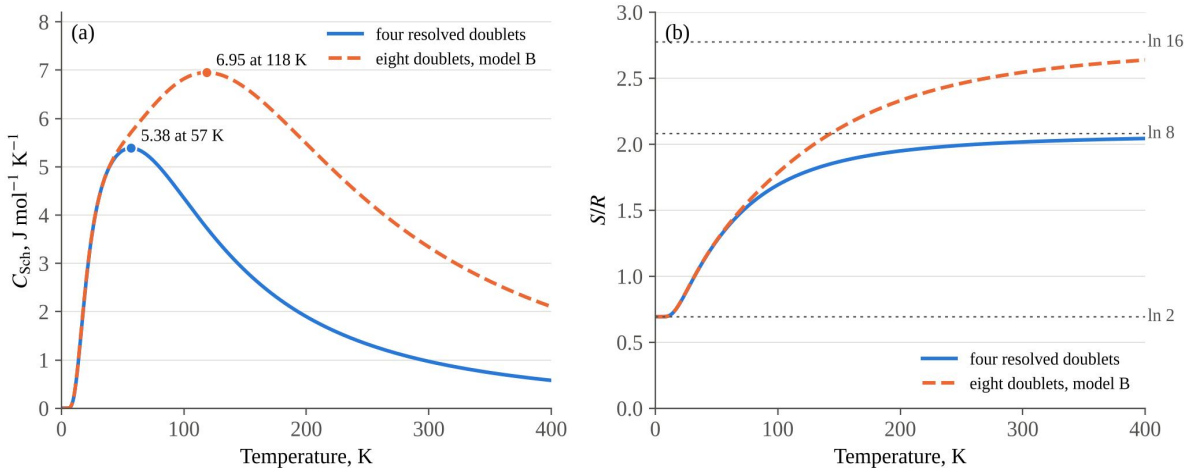


Figure 3. Single-ion Schottky heat capacity (a) and magnetic entropy (b) of Dy^{3+} in $DyAlO_3$, calculated for the four resolved doublets and for the complete eight-doublet scheme of model B. Calculated by the authors.

Table 6. Schottky heat capacity and magnetic entropy of Dy^{3+} in $DyAlO_3$

T, K	C_{Sch} (4 doublets), J mol^{-1} K^{-1}	C_{Sch} (model B), J mol^{-1} K^{-1}	S/R (4 doublets)	S/R (model B)
4.2	0.00	0.00	0.693	0.693
20	2.58	2.60	0.795	0.796
50	5.33	5.48	1.267	1.271
77	5.08	6.32	1.543	1.576
100	4.35	6.82	1.692	1.783
150	2.85	6.64	1.868	2.118
300	0.97	3.34	2.017	2.545

Source: calculated by the authors with Eq. (6); limits: ln 2 = 0.693, ln 8 = 2.079, ln 16 = 2.773.

Magnetization. Figure 4 and Table 7 compare the magnetization at 10 K calculated with Eq. (7). Along its axis, the Ising doublet magnetizes much more easily than a free ion with the same saturation moment: at 1 T it reaches 5.87 μ_B, 2.4 times the free-ion value (2.46 μ_B), and at 5 T it

ISSN: 2224-6878 | Pakistan Volume 6, No. 10.

IF: 14.91 | 2026 http://waerasia.org/index.php/ijtar

is practically saturated (9.98 μ_B). Averaged over field directions, the Ising doublet saturates at only half of $g_J J\mu_B$, i.e. 5 μ_B, because the moment can point only along the local axis and its projection on the field averages to $\langle |\cos\theta| \rangle = 1/2$.

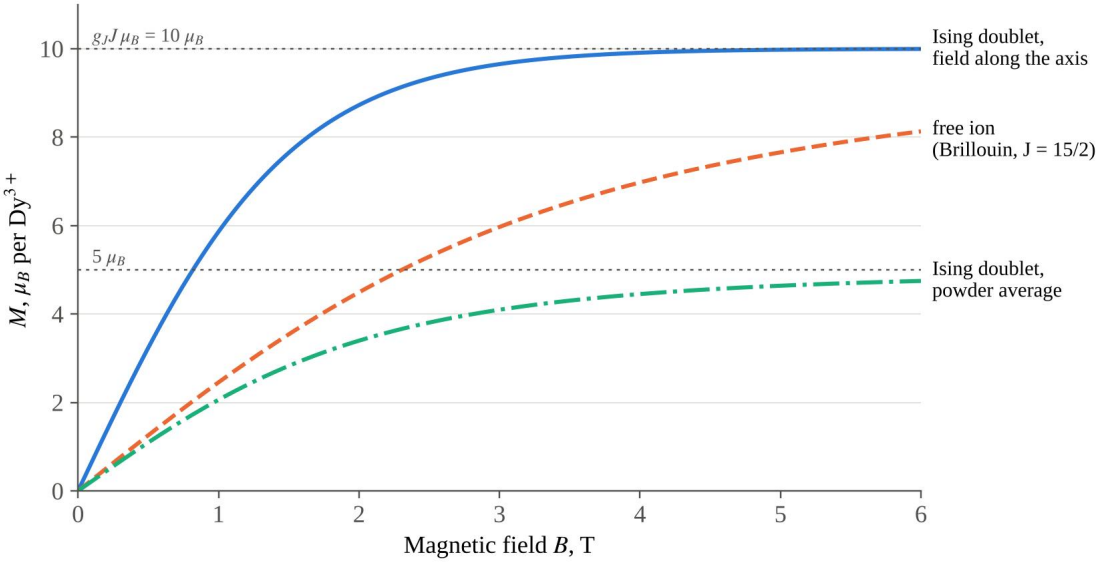


Figure 4. Magnetization of Dy^{3+} at T = 10 K: Ising $|\pm 15/2\rangle$ doublet with the field along its axis, free ion (Brillouin function, J = 15/2) and Ising doublet averaged over field directions. Calculated by the authors, exchange neglected.

Table 7. Magnetization of Dy^{3+} (μ_B per ion) at T = 10 K

B, T	Ising doublet, field along the axis	Free ion (J = 15/2)	Ising doublet, powder average
0.5	3.25	1.26	1.10
1	5.87	2.46	2.06
2	8.73	4.50	3.40
5	9.98	7.66	4.64
$\to \infty$	10.00	10.00	5.00

Source: calculated by the authors with Eq. (7).

Discussion. What the axial fit shows. The effective axial model is deliberately minimal, and its value lies in what it rules out. A pure second-order field cannot reproduce the spacing of the four lowest doublets, so the CF acting on Dy^{3+} in $DyAlO_3$ cannot be reduced to its uniaxial B_2^0 component, although that component determines the sign of the anisotropy. A small fourth-order term ($B_4^0 O_4^0$ reaches tens of cm^{-1} at large M because O_4^0 scales as M^4) is enough to reproduce the observed intervals. Two caveats limit the interpretation. With one degree of freedom, the near-perfect fit of model B shows that the data are consistent with an axial description, not that the description is unique; the sixth-order term B_6^0 and the non-axial terms allowed by C_s symmetry could produce a similar pattern. Moreover, the non-axial terms mix $|M\rangle$ states, so the doublets are only approximately $|\pm M\rangle$. For the ground doublet, the agreement with the Ising picture established from magnetic and optical data [1, 6] shows that this mixing is small.

Link with magnetic anisotropy. In the axial model, doublets II–IV ($|\pm 13/2\rangle$, $|\pm 11/2\rangle$, $|\pm 9/2\rangle$) are themselves Ising-like, with $g_{\parallel}$ = 17.3, 14.7 and 12.0 and $g_{\perp} = 0$. Because these doublets are significantly populated at 77–300 K, the model explains why the susceptibility of

ISSN: 2224-6878 | Pakistan Volume 6, No. 10.

IF: 14.91 | 2026 http://waerasia.org/index.php/ijtar

$DyAlO_3$ stays strongly anisotropic above 100 K [1] without additional assumptions. The anisotropy should weaken noticeably only when the $|\pm 3/2\rangle$ and $|\pm 1/2\rangle$ doublets become populated. The $|\pm 1/2\rangle$ doublet has $g_\perp = g_J(J + 1/2) = 10.7$, i.e. easy-plane character, and is predicted at about 416 cm^{-1}, i.e. at temperatures of several hundred kelvin. The van Vleck contribution, which arises from field-induced mixing of excited states into the ground state, controls the susceptibility perpendicular to the Ising axis [14, 15] and can be calculated directly from the model B wave functions.

Calorimetric test. The heat capacity offers the most direct test of the predicted upper levels. Up to about 40 K, C_{Sch} depends only on the resolved doublets and is fixed by the data; above 60 K it depends almost entirely on doublets V–VIII. A measurement of the heat capacity of $DyAlO_3$, with the lattice contribution subtracted using an isostructural non-magnetic orthoaluminate as reference, should show a Schottky maximum near 118 K if model B is correct and near 57 K if the upper doublets lie much higher. The magnetic entropy offers the same test in integral form: S/R at 150 K is 2.12 in model B against 1.87 for the truncated scheme.

Implications for magnetic cooling. Below 20 K the entropy of $DyAlO_3$ is within 15% of R ln 2 (Table 6), so the full Kramers-doublet entropy is available for field-induced changes, while the next doublet lies 77 K higher and does not add parasitic heat capacity. Together with the easy saturation of the Ising moment along its axis (Table 7), this justifies considering $DyAlO_3$ single crystals as working bodies for magnetic refrigeration in the liquid-helium to liquid-hydrogen range. The magnetization results also show that crystal orientation matters: a randomly oriented polycrystal saturates at only half the moment of an oriented crystal.

Limitations. The analysis rests on four measured doublet energies and an assumed $|M\rangle$ assignment. Exchange and dipolar interactions between Dy^{3+} ions, which cause magnetic ordering at low temperature, were neglected, so the magnetization curves apply to the paramagnetic regime. The fitted parameters are effective axial parameters, not the full set of C_s CF parameters. Resolving the upper doublets spectroscopically, for example in hot bands at 150–300 K or in the $^6H_{15/2} \rightarrow {}^6F_{5/2}$ band, and fitting the complete CF Hamiltonian jointly to optical, magnetic and calorimetric data are the natural next steps.

Conclusion. The study gives a quantitative single-ion description of Dy^{3+} in $DyAlO_3$:

1. Hund's rules give the ground term $^6H_{15/2}$ with $g_J = 4/3$, $\mu_{eff} = 10.65\ \mu_B$ and $\mu_{sat} = 10\ \mu_B$. The effective moment is the highest among the trivalent lanthanides, and as a Kramers ion Dy^{3+} keeps doublet ground states in any crystal field.

2. The energies of the four lowest doublets (0, 53.7, 125.7, 205.5 cm^{-1}) cannot be described by a second-order axial field (rms 16.1 cm^{-1}) but are reproduced within 0.3 cm^{-1} with $B_2^0 = -2.55$ cm^{-1} and $B_4^0 = 2.45\times10^{-3}$ cm^{-1}. The negative B_2^0 confirms the Ising ground doublet $|\pm 15/2\rangle$ ($g_{\parallel} = 20$, $g_\perp = 0$).

3. The model predicts doublets V–VIII at 281, 345, 392 and 416 cm^{-1}, a total splitting of about 416 cm^{-1}, and Ising-like character for all doublets up to $|\pm 3/2\rangle$, which explains the persistence of magnetic anisotropy above 100 K.

4. The Schottky maximum is predicted at 118 K (6.95 J mol^{-1} K^{-1}) for the complete scheme and at 57 K (5.38 J mol^{-1} K^{-1}) for the resolved doublets only, which provides a calorimetric test of the predicted levels; below 20 K the magnetic entropy is close to R ln 2.

5. At 10 K and 1 T, the Ising doublet gives 5.87 μ_B along its axis, compared with 2.46 μ_B for a free ion and 2.06 μ_B for a powder, which supports the use of oriented $DyAlO_3$ crystals in low-temperature magnetic cooling.

ISSN: 2224-6878 | Pakistan Volume 6, No. 10.

IF: 14.91 | 2026 http://waerasia.org/index.php/ijtar

REFERENCES

1. Valiev U.V., Dzhuraev D.R., Malyshev E.E., Saidov K.S. Electronic structure of the ground multiplet of the Dy^{3+} ion in $DyAlO_3$ orthoaluminate // Optika i Spektroskopiya. 1999. Vol. 86, No. 5. P. 789–793 (in Russian).
2. Wybourne B.G. Spectroscopic Properties of Rare Earths. New York: Interscience Publishers, 1965. 236 p.
3. Abragam A., Bleaney B. Electron Paramagnetic Resonance of Transition Ions. Oxford: Clarendon Press, 1970. 911 p.
4. Hutchings M.T. Point-charge calculations of energy levels of magnetic ions in crystalline electric fields // Solid State Physics. 1964. Vol. 16. P. 227–273.
5. Kramers H.A. Théorie générale de la rotation paramagnétique dans les cristaux // Proceedings of the Royal Netherlands Academy of Arts and Sciences. 1930. Vol. 33. P. 959–972.
6. Elliott R.J., Stevens K.W.H. The theory of magnetic resonance experiments on salts of the rare earths // Proceedings of the Royal Society A. 1953. Vol. 218. P. 553–566.
7. Bleaney B., Stevens K.W.H. Paramagnetic resonance // Reports on Progress in Physics. 1953. Vol. 16. P. 108–159.
8. Hund F. Linienspektren und periodisches System der Elemente. Berlin: Springer, 1927.
9. Carnall W.T., Fields P.R., Rajnak K. Electronic energy levels in the trivalent lanthanide aquo ions. I. Pr^{3+}, Nd^{3+}, Pm^{3+}, Sm^{3+}, Dy^{3+}, Ho^{3+}, Er^{3+}, and Tm^{3+} // Journal of Chemical Physics. 1968. Vol. 49, No. 10. P. 4424–4442. DOI: 10.1063/1.1669893.
10. Dieke G.H. Spectra and Energy Levels of Rare Earth Ions in Crystals. New York: Interscience Publishers, 1968. 401 p.
11. Stevens K.W.H. Matrix elements and operator equivalents connected with the magnetic properties of rare earth ions // Proceedings of the Physical Society A. 1952. Vol. 65. P. 209–215.
12. Tari A. The Specific Heat of Matter at Low Temperatures. London: Imperial College Press, 2003.
13. Van Vleck J.H. The Theory of Electric and Magnetic Susceptibilities. Oxford: Oxford University Press, 1932. 384 p.
14. Valiev U.V., Gruber J.B., Sardar D., Zandi B., Kachur I.S., Mukhammadiev A.K., Piryatinskaya V.G., Sokolov V.Yu., Edelman I.S. Zeeman effect and features of the Stark splitting of electronic states of the rare-earth ion in terbium paramagnetic garnets $Tb_3Ga_5O_{12}$ and $Tb_3Al_5O_{12}$ // Fizika Tverdogo Tela. 2007. Vol. 49, No. 1. P. 87–94 (in Russian).